JACS
JOURNAL OF THE AMERICAN CHEMICAL SOCIETY
Article
pubs.acs.org/JACS

Highly Selective, Reversible Inhibitor Identified by Comparative Chemoproteomics Modulates Diacylglycerol Lipase Activity in Neurons

Marc P. Baggelaar,[†] Pascal J. P. Chameau,[‡] Vasudev Kantae,[§] Jessica Hummel,[†] Ku-Lung Hsu,[∥,#] Freek Janssen,[†] Tom van der Wel,[†] Marjolein Soethoudt,[†] Hui Deng,[†] Hans den Dulk,[†] Marco Allarà,[⊥] Bogdan I. Florea,[†] Vincenzo Di Marzo,[⊥] Wytse J. Wadman,[‡] Chris G. Kruse,[‡] Herman S. Overkleeft,[†] Thomas Hankemeier,[§] Taco R. Werkman,[‡] Benjamin F. Cravatt,[∥] and Mario van der Stelt*[,†]

[†]Department of Bioorganic Synthesis, Leiden Institute of Chemistry, Leiden University, Leiden 2300 RA, The Netherlands
[‡]Center for Neuroscience, Swammerdam Institute for Life Sciences, University of Amsterdam, Amsterdam 1000 GG, The Netherlands
[§]Division of Analytical Biosciences, Leiden Academic Centre for Drug Research, Leiden University, Leiden 2300 RA, The Netherlands
[∥]Department of Chemical Physiology, The Scripps Research Institute, La Jolla, California 92037, United States
[⊥]Endocannabinoid Research Group, Institute of Biomolecular Chemistry, Pozzuoli 80078, Italy

Supporting Information

ABSTRACT: Diacylglycerol lipase (DAGL)-α and -β are enzymes responsible for the biosynthesis of the endocannabinoid 2-arachidonoylglycerol (2-AG). Selective and reversible inhibitors are required to study the function of DAGLs in neuronal cells in an acute and temporal fashion, but they are currently lacking. Here, we describe the identification of a highly selective DAGL inhibitor using structure-guided and a chemoproteomics strategy to characterize the selectivity of the inhibitor in complex proteomes. Key to the success of this approach is the use of comparative and competitive activity-based proteome profiling (ABPP), in which broad-spectrum and tailor-made activity-based probes are combined to report on the inhibition of a protein family in its native environment. Competitive ABPP with broad-spectrum fluorophosphonate-based probes and specific β-lactone-based probes led to the discovery of α-ketoheterocycle LEI105 as a potent, highly selective, and reversible dual DAGL-α/DAGL-β inhibitor. LEI105 did not affect other enzymes involved in endocannabinoid metabolism including abhydrolase domain-containing protein 6, abhydrolase domain-containing protein 12, monoacylglycerol lipase, and fatty acid amide hydrolase and did not display affinity for the cannabinoid CB_1 receptor. Targeted lipidomics revealed that LEI105 concentration-dependently reduced 2-AG levels, but not anandamide levels, in Neuro2A cells. We show that cannabinoid CB_1-receptor-mediated short-term synaptic plasticity in a mouse hippocampal slice model can be reduced by LEI105. Thus, we have developed a highly selective DAGL inhibitor and provide new pharmacological evidence to support the hypothesis that "on demand biosynthesis" of 2-AG is responsible for retrograde signaling.

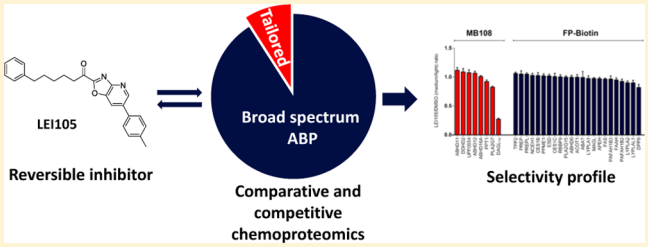

INTRODUCTION

Endocannabinoids are endogenous signaling lipids that activate the cannabinoid CB_1 and CB_2 receptor. They play an essential role in human health and disease, regulating processes such as immunomodulation, energy balance and neurotransmission.[1] There are two main endocannabinoids: anandamide and 2-arachidonoylglycerol (2-AG).[2−4] Both endocannabinoids are often found together, but their levels vary between species, tissue type, developmental stage, and pathological condition.[5] Although selective inhibitors of their metabolic pathways have provided information about the biological function of the endocannabinoids, it is still unclear to a large extent which endocannabinoid is responsible for specific cannabinoid CB_1 receptor dependent (patho)physiological effects.[6,7] Selective inhibition of the formation of anandamide and 2-AG would be instrumental to determine which endocannabinoid is responsible for specific CB_1-mediated physiological effects. However, pathway-selective inhibitors for 2-AG and anandamide biosynthesis are currently lacking.

2-AG is mainly formed by the action of two diacylglycerol lipases (DAGL-α and DAGL-β).[8] DAGLs are intracellular, multidomain integral membrane proteins. The DAGLs share extensive homology, but differ in size: ∼120 and ∼70 kDa for

Received: May 11, 2015
Published: June 17, 2015

DOI: 10.1021/jacs.5b04883
J. Am. Chem. Soc. 2015, 137, 8851−8857

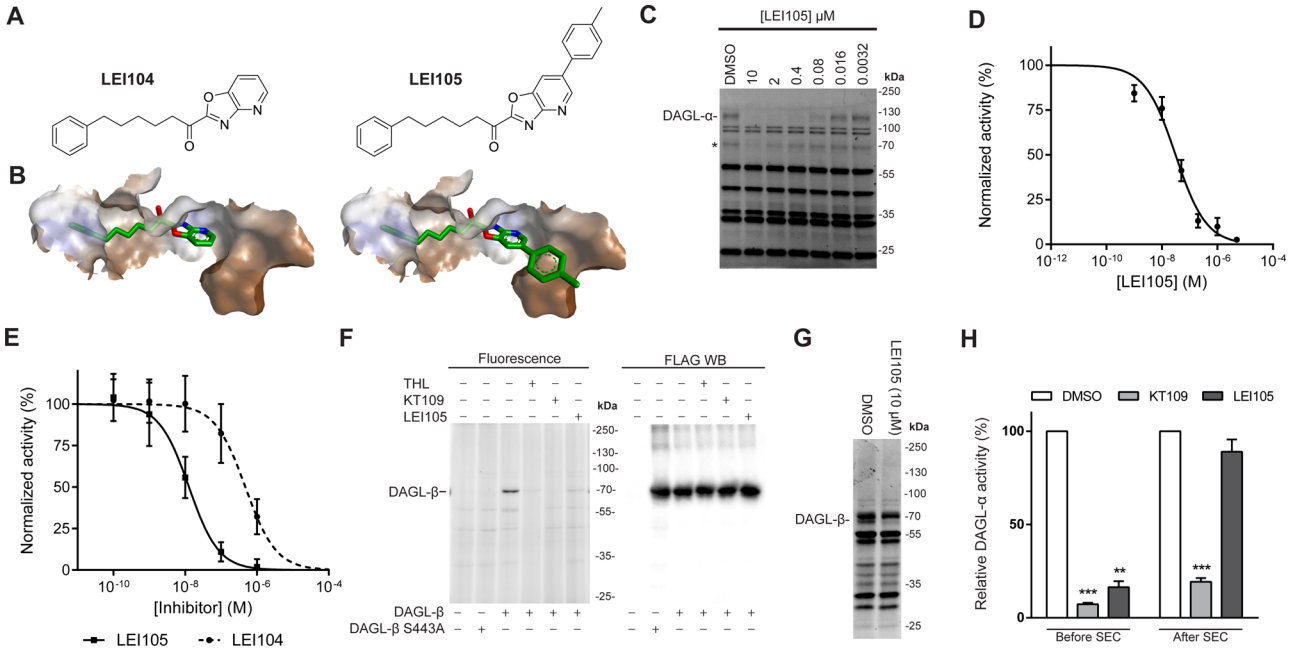

Figure 1. Structure-guided modeling and biochemical characterization of LEI105. (a) Structures of α-ketoheterocycle based DAGL inhibitors LEI104 and LEI105. (b) LEI104 and LEI105 in a homology model of DAGL-α. (c) Representative fluorescent ABPP gel showing dose dependent inhibition of MB064 (250 nM) labeling of endogenous DAGL-α labeling by LEI105 in the mouse brain membrane proteome. (* = DAGL-α breakdown product) (d) Dose response curve of DAGL-α inhibition as determined with competitive ABPP (pIC_{50} 7.5 ± 0.07 (IC_{50} = 32 nM); n = 3). (e) Dose response curve of DAGL-α inhibition by LEI104 (pIC_{50} 6.3 ± 0.1 (IC_{50} = 501 nM); n = 4) and LEI105 (pIC_{50} 7.9 ± 0.08 nM (IC_{50} = 13 nM); n = 4) as determined with a glycerol based natural substrate assay. (f) ABPP using MB064 (1 μM) with different hDAGL-β constructs and anti-FLAG Western blot of the same gel. (g) Competitive ABPP in the mouse spleen membrane proteome using MB064 (1.0 μM) in competition with LEI105 (10 μM), LEI105 can block labeling of endogenously expressed DAGL-β in the mouse spleen membrane proteome. (H) Schematic representation of the size exclusion chromatography (SEC) experiment that shows reversibility of LEI105 in recombinant DAGL-α (n = 3, full fluorescent gel and Western blot are given in the Supporting Information, SI) Statistical analysis: 2-way ANOVA (*** = $p < 0.001$; ** = $p < 0.01$ vs vehicle).

DAGL-α and DAGL-β, respectively.[8,9] DAGLs belong to the class of serine hydrolases that employ the typical Ser-His-Asp catalytic triad to hydrolyze the ester bond of acyl chains from arachidonate-containing diacylglycerols in a *sn*-1 specific manner. Studies with DAGL knockout mice have shown that DAGL-α controls to a large extent the formation of 2-AG in the central nervous system, whereas DAGL-β appears to partake in 2-AG production in the periphery during inflammation.[5,10] Importantly, also basal anandamide levels were reduced in DAGL-α knockout mice. Selective inhibitors for DAGLs, which can be used in an acute and temporal fashion and do not modulate anandamide levels, would, therefore, constitute an important counterpart of the DAGL knockout mice, and allow the examination of acute versus congenital inhibition.

Although, several classes of DAGL inhibitors have been described in literature,[8,11−15] these inhibitors are based on the natural substrates and/or have reactive chemical warheads, and are not selective over other serine hydrolases that modulate endocannabinoid signaling (e.g., abhydrolase domain-containing protein 6 and 12 (ABHD6 and ABHD12), monoacylglycerol lipase (MAGL), or fatty acid amide hydrolase (FAAH)), therefore highly selective DAGL inhibitors are warranted to study the cellular role of the biosynthetic enzymes.

Activity-based protein profiling (ABPP) has emerged as a powerful technique for discovering selective enzyme inhibitors acting in their native physiological context.[16] ABPP hinges on the use of activity-based probes (ABPs) to report on enzyme activity in cells, tissue or animals.[17] An ABP normally consists of a covalent, irreversible enzyme inhibitor featuring a reporter entity (fluorophore, biotin, bioorthogonal tag) to label the active site of the enzyme or enzyme family at hand. ABPP is unique in its ability to rapidly identify inhibitor activity and selectivity within large enzyme families in complex proteome samples. The prototypical ABP for serine hydrolases is based on a fluorophosphonate (FP)-warhead.[18] However, this probe does not recognize DAGL-α, and the signals for DAGL-β, MAGL, and ABHD6 cannot be unequivocally established because not all gel bands can be clearly resolved in the brain proteome.[19] Previously, we have reported on the design, synthesis, and characterization of a specific β-lactone-containing probe (MB064), which was tailor-made for the detection of DAGL-α activity.[20,21] Using this probe, we identified 1-(oxazolo[4,5-*b*]pyridin-2-yl)-6-phenylhexan-1-one (LEI104, Figure 1), which belongs to the class of α-ketoheterocycles, as the first reversible inhibitor for DAGL-α. LEI104 was, however, weakly active in a cellular assay and was not selective over FAAH, the enzyme responsible for the metabolism of the other endocannabinoid anandamide (AEA).[22,23] Moreover, activity of LEI104 on DAGL-β was not studied, but in view of the high homology between DAGL-α and DAGL-β, it is likely that there is cross-reactivity. In order to apply α-ketoheterocycles as chemical tools to study 2-AG signaling, it is important to increase their cellular activity, to have selectivity over FAAH and to assess their activity on endogenous DAGL-β.

Here, we report a structure-guided approach to optimize LEI104 employing a homology-model of DAGL-α. In addition, we discovered that our tailor-made β-lactone probe MB064

DOI: 10.1021/jacs.5b04883
J. Am. Chem. Soc. 2015, 137, 8851−8857

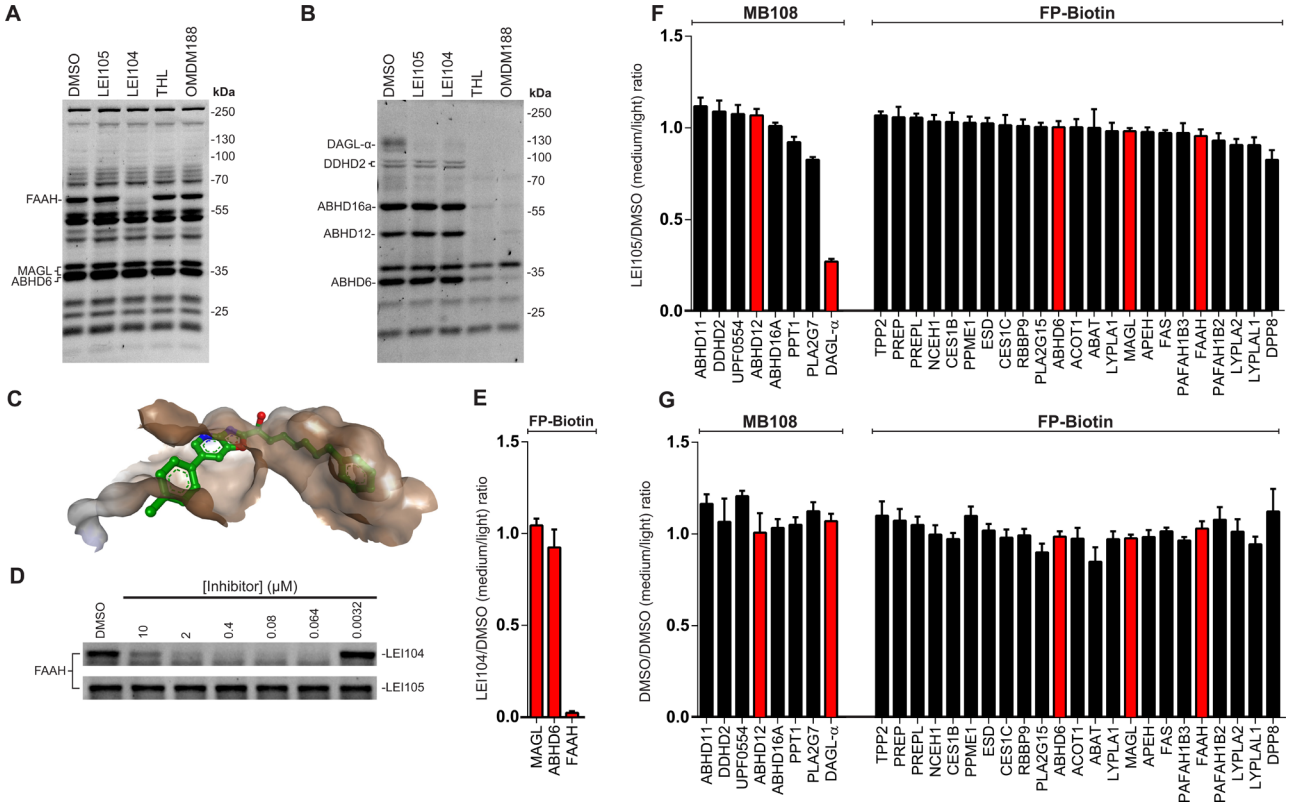

Figure 2. Selectivity of LEI105. (a) Competitive ABPP in the mouse brain membrane proteome with LEI104 (10 μM), LEI105 (10 μM), OMDM188 (1 μM), and THL (1 μM) using TAMRA-FP (500 nM). (b) Same experiment as in (a) with THL based ABP MB064 (250 nM) showing excellent selectivity of LEI105 at 10 μM compared to THL and OMDM188. (c) One possible LEI105-like conformer in a previously reported cocrystal structure of FAAH, showing a steric clash between the toluyl group and FAAH. (d) Activity of LEI104 and LEI105 against FAAH in a concentration response experiment in the mouse brain membrane proteome using TAMRA-FP (500 nM, full gels are given in the SI). (e) Chemoproteomic competition between LEI104 (10 μM) and FP-biotin (5 μm) for FAAH, MAGL, and ABHD6, showing that the chemoproteomic settings using FP-biotin are compatible with reversible α-ketoheterocycles. (f) MB108 and FP-biotin based chemoproteomic analysis of serine hydrolase activities in the mouse brain membrane proteome treated with LEI105 (10 μM). DAGL-α labeling is reduced to over 70%. (g) Chemoproteomic control experiment shows equal isotopic labeling and detection of peptides from MB108 and FP-biotin labeled serine hydrolases. Enzymes known to be directly involved in endocannabinoid biosynthesis and metabolism are highlighted in red. (n = 3–4 independent chemoproteomics experiments; Error bars represent ± s.e.m. of medium over light ratios of quantified peptides (minimum of two unique peptides per enzyme). Only unique proteins are given for MB108, all detected proteins including proteins overlapping between the probes are given in the SI. See SI data set **1** for complete proteomic data.

could also label DAGL-β in cells and tissues. Using these tools, we characterized LEI105 as a cellular active, dual DAGL-α/β inhibitor. Comparative chemoproteomics revealed that LEI105 is selective over ABHD6, ABHD12, MAGL, and FAAH. Furthermore, targeted lipidomics revealed that LEI105 is able to concentration-dependently reduce 2-AG levels in neuronal cells without affecting AEA levels. We showed that cannabinoid CB_1-receptor-dependent short-term synaptic plasticity in a hippocampal slice model can be reduced by the selective DAGL-inhibitor LEI105. In summary, comparative and competitive chemoproteomics were applied to characterize the most selective DAGL inhibitor to date, that can be used to study DAGL function in an acute and temporal manner in a neuronal context.

RESULTS AND DISCUSSION

Structure-Guided Modeling to Identify LEI105 as DAGL-α Inhibitor. Previously, we have identified the α-ketoheterocycle, 1-(oxazolo[4,5-*b*]pyridin-2-yl)-6-phenylhexan-1-one (LEI104, Figure 1A), as an inhibitor for DAGL-α. To improve the potency of LEI104 (Figure 1A) we used a structure-guided modeling approach. We investigated in detail the binding pose of LEI104 in DAGL-α using a molecular dynamics simulation in our previously generated homology model.[21] From this analysis, we identified an additional hydrophobic pocket close to the catalytic site that did not appear to be occupied by LEI104 (Figure 1B). Introduction of a phenyl substituent at the 6-position of the oxazolopyridine would allow us to probe this pocket with the aim of increasing potency and/or selectivity. We synthesized compound (LEI105) (see SI for synthesis) and tested its activity on human DAGL-α in a colorimetric assay using *para*-nitrophenylbutyrate as a surrogate substrate.[24] LEI105 proved to be a potent inhibitor with a pIC_{50} of 8.5 ± 0.06 (n = 4), thus some 10-fold more potent than LEI104 (7.4 ± 0.05; n = 4).[21] Reduction of the α-keto group to the corresponding alcohol (compound **8** (SI)) led to a ~150 fold drop of activity against DAGL-α, thereby indicating that the α-carbonyl in LEI105 reacts with the active site serine hydroxyl to form a covalent, though reversible, enzyme–inhibitor hemiketal adduct. To confirm that LEI105 was also able to block conversion of the natural substrate 1-stearoyl-2-arachidonoyl-*sn*-glycerol of DAGL-α to the endocannabinoid 2-AG, we employed our recently developed real-time, fluorescence-based assay.[25] In this

DOI: 10.1021/jacs.5b04883
J. Am. Chem. Soc. 2015, 137, 8851–8857

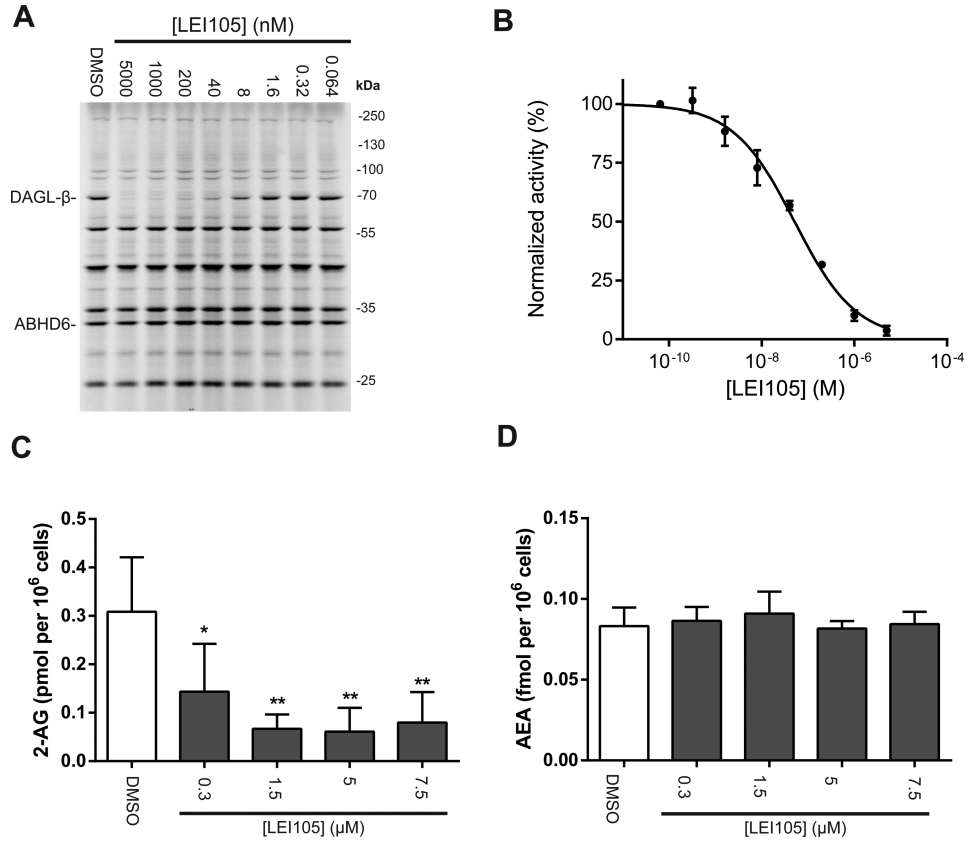

Figure 3. Cellular activity of LEI105. (a) Representative gel of concentration-dependent inhibition of endogenous DAGL-β in vitro in the Neuro2A proteome as determined with ABP MB064. (b) Dose response curve of DAGL-β inhibition as determined with competitive ABP MB064 (±SEM, n = 3). (c) In situ treatment of Neuro2A cells (1 h, 37 °C) dose dependently decreased basal 2-AG levels while keeping anandamide (AEA) levels (d) constant (mean ± SEM; n = 4). Statistical analysis: 2-way ANOVA (*** = $p < 0.001$; ** = $p < 0.01$; and * = $p < 0.05$ vs vehicle).

assay, LEI105 inhibited recombinant human DAGL-α with a pIC_{50} of 7.9 ± 0.08 (n = 4) (Figure 1E), which is a 40-fold increase compared to LEI104 (pIC_{50} 6.3 ± 0.1 (n = 4)). The inhibitory activity of LEI105 was confirmed in a radiometric assay using 1-[^{14}C]oleoyl-2-arachidonoyl-*sn*-glycerol (1.0 mCi mmol^{-1}, 20 μm) as substrate (pIC_{50} of 6.6; n = 2).[8]

Determining Endogenous DAGL Activity Using MB064 as ABP. To test the activity of LEI105 on endogenously expressed DAGL-α in mouse membrane proteome, we used our previously reported ABPP method with MB064.[21] Eleven tissues from wild-type and DAGL-α knockout mice were screened to obtain a tissue-wide profile of endogenous DAGL-α activity (SI). DAGL-α activity was found to be highest in the brain (which is in line with our previous reported results on a smaller set of tissues).[21] LEI105 prevented DAGL-α labeling in the mouse brain membrane proteome by MB064 with a pIC_{50} of 7.5 ± 0.07 (n = 3) (Figure 1C, D).

In view of the high homology between DAGL-α and DAGL-β, we assessed the activity of LEI105 also on native DAGL-β. To this end, we tested whether our ABP MB064 was also able to label DAGL-β. We incubated MB064 with membranes from mock and hDAGL-β transfected HEK293T cells. MB064 labeled a protein at the expected molecular weight of DAGL-β, which was not present in the control membranes, or in S443A-hDAGL-β transfected cells, in which the catalytic serine is replaced by alanine using site-directed mutagenesis (Figure 1F). Thus, our tailor-made probe can also detect DAGL-β. Labeling of hDAGL-β was inhibited by LEI105 with a pIC_{50} of 7.4 ± 0.07 (n = 3) (SI). We confirmed the activity of LEI105 on human DAGL-β using a biochemical assay with *para*-nitrophenylbutyrate as a surrogate substrate (pIC_{50} of 8.1 ± 0.07, n = 4; SI). Next, we used the MB064 ABP to profile endogenous DAGL-β activity in 12 tissues from wild-type and DAGL-β knockout mice. Spleen tissue was found to display the highest DAGL-β activity. This activity could be inhibited by LEI105 (Figure 1G). Of note, we could not detect DAGL-β activity with MB064 in the brain.

To determine the mode of action (reversible versus irreversible) of LEI105, we performed an experiment in which human DAGL-α membranes were preincubated at the IC_{80} concentration of LEI105 or the irreversible DAGL inhibitor KT-109.[15] The protein was separated from small molecule inhibitors via size exclusion column chromatography and remaining enzyme activity was visualized with MB064. No recovery of DAGL-α activity was found for KT-109, whereas MB064 labeled DAGL-α exposed to LEI105 with similar intensity to DMSO treated DAGL-α (Figure 1H). This indicates that LEI105 is a reversible inhibitor of DAGL-α.

Determining Proteome-Wide Selectivity of LEI105 Using Comparative and Competitive Chemoproteomics. To investigate the selectivity of LEI105 in the mouse brain proteome, we have used comparative and competitive ABPP with a broad-spectrum FP-based probe (TAMRA-FP) and the tailored DAGL-α ABP MB064. As a reference, we first tested the widely used β-lactone-based DAGL-inhibitors THL and OMDM-188, two highly potent nonselective covalent and irreversible serine hydrolase inhibitors.[8,14] In our experimental setup, both compounds blocked labeling of at least 4 serine

DOI: 10.1021/jacs.5b04883
J. Am. Chem. Soc. 2015, 137, 8851−8857

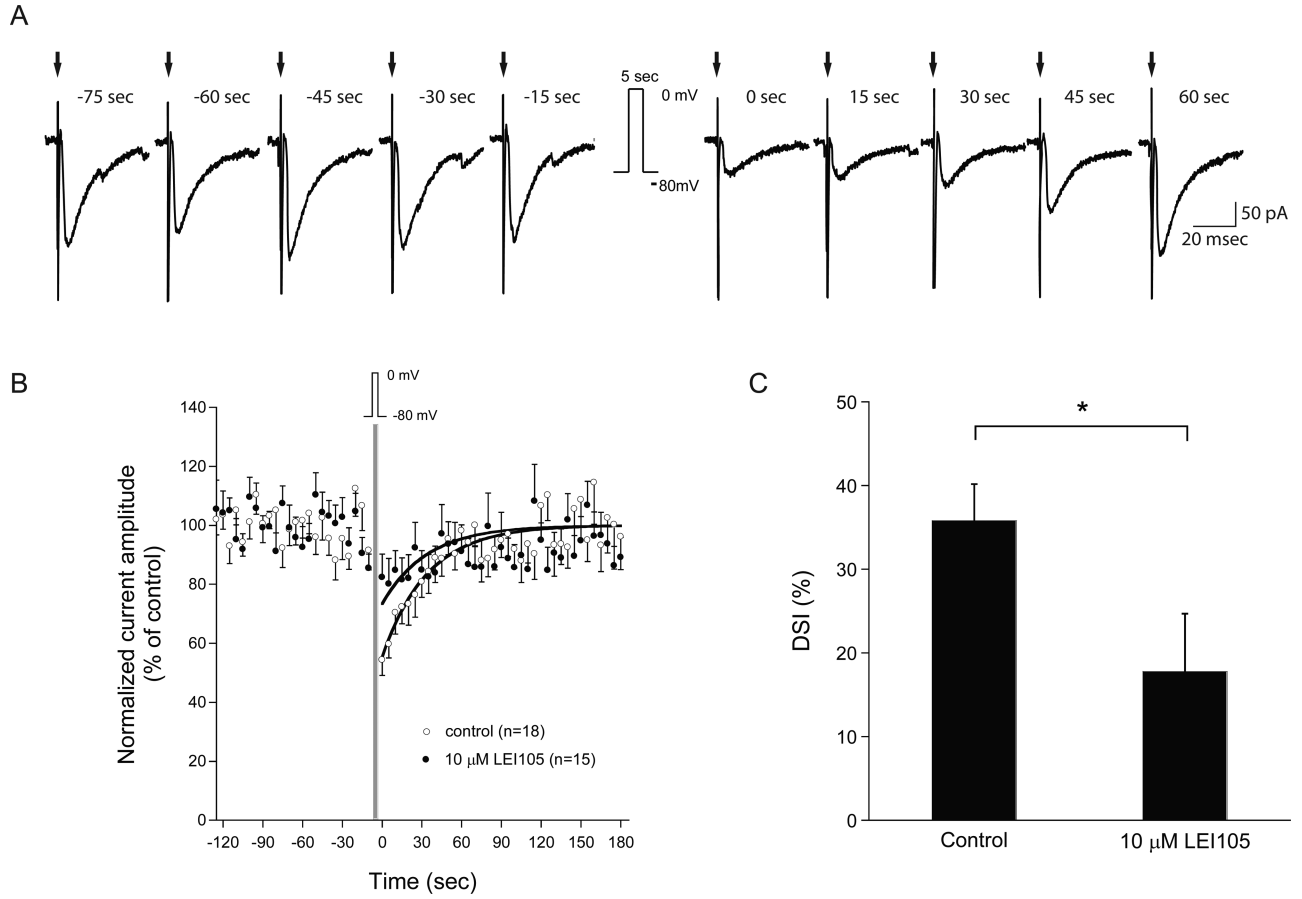

Figure 4. DSI is reduced in hippocampal slices treated with 10 μM LEI015. (a) Example of a typical whole-cell voltage-clamp recording of evoked inhibitory postsynaptic currents (IPSCs) in a CA1 pyramidal neuron under control conditions. IPSCs are evoked every 5 s, but for clarity, IPSCs shown here are representative traces recorded every 15 s. DSI is induced with a 5-s duration depolarization from −80 to 0 mV and is observed as a marked and brief reduction of IPSC amplitude following the depolarization. (b) Averaged IPSC amplitude recorded every 5 s in CA1 neurons from vehicle-treated slices (DMSO) and from slices preincubated at least 30 min and in the continuous presence of LEI 105 (10 μM). The dark lines represent the single exponential fit of the recovery phase following the depolarizing step. (c) Initial DSI amplitude under control conditions (DMSO) and in the presence of LEI105 (10 μM). (* $p < 0.05$ vs vehicle).

hydrolases at concentrations as low as 1 μM, including ABHD6 and ABHD12, enzymes involved in 2-AG metabolism in the brain (Figure 2A, B).

In our previous studies, we identified fatty acid amide hydrolase (FAAH) as a major off-target for LEI104. In stark contrast to LEI104, which inhibited FAAH labeling with a pIC_{50} of 7.8 ± 0.04 (n = 3) (Figure 2D, SI), LEI105 did not block FAAH labeling up to a concentration of 10 μM (n = 3) (Figure 2A, D). Of note, LEI105 did not inhibit labeling of any other band either, and we conclude that LEI105 is highly selective at least within the panel of serine hydrolases labeled by TAMRA-FP and MB064. To explain this remarkable selectivity of LEI105 over FAAH, we looked in detail into a previously published cocrystal structure of FAAH with OL-135 (pdb: 2WJ1 and 2WJ2).[26] In silico modification of the heterocyclic part of OL-135, in the presence of the protein, to a LEI105 like conformer revealed a steric clash of the toluoyl moiety of LEI105 with the substrate channel of FAAH, thereby possibly explaining the high selectivity of LEI105 over FAAH compared to its analog LEI104 (Figure 2C).

Since, the human serine hydrolase family contains approximately 200 family members,[27] we wanted to examine the selectivity of LEI105 in the brain proteome in a broader and more detailed manner. To this end, we adapted a semi-quantitative chemoproteomics protocol, which was previously applied to determine the selectivity profile of the irreversible inhibitor KT-109, using MB108, a biotinylated version of MB064 and the FP-probe (see SI for synthesis and characterization). This methodology allows for a more accurate quantification avoiding band overlap (as observed with gel-based assay) and enables screening over a broader range of specified serine hydrolases. We first validated equal isotopic labeling and detection of light and medium peptides from proteins targeted by both ABPs (Figure 2G). Next, we set out to investigate the selectivity of LEI105 in this chemoproteomic assay. LEI105 (10 μM, 30 min) did not reduce labeling of the detected serine hydrolases by more than 20%, except for DAGL-α (Figure 2F). In addition, we tested LEI105 in biochemical assays using recombinant human ABHD6 and MAGL and in a cannabinoid CB_1 receptor radioligand displacement assay. We did not find any significant interaction ($pK_i < 5$) with these proteins of the endocannabinoid system (SI). Together, these results indicate that LEI105 is a highly selective DAGL-inhibitor.

LEI105 Reduces 2-AG Levels in Neuro2A Cells. To test the cellular activity of LEI105, we used Neuro2A cells, which is a mouse neuroblastoma cell line known to express both DAGL-α and DAGL-β.[28] First, we confirmed the presence of the

DOI: 10.1021/jacs.5b04883
J. Am. Chem. Soc. 2015, 137, 8851−8857

mRNA transcripts of both DAGLs. Interestingly, we found that DAGL-β mRNA levels are ~128-fold higher, compared to DAGL-α, as determined by qPCR (SI). In line, DAGL-α protein activity was below the detection limit of our ABPP assay, whereas we detected a fluorescent band at the expected molecular weight of DAGL-β using MB064 (Figure 3A; SI for validation of DAGL-β labeling). LEI105 selectively reduced DAGL-β labeling in a concentration dependent manner with a pIC_{50} of 7.3 ± 0.07 (Figure 3A, B). Of note, no inhibition of ABHD6 or FAAH was observed (SI). Next, in a targeted lipidomics experiment, we determined the effect of LEI105 on the cellular levels of 2-AG and anandamide. A concentration-dependent reduction of 2-AG was found in Neuro2A cells, whereas anandamide levels were unaffected (Figure 3C, D). To test the activity of LEI105 in a human cell line, we used human PC3 cells. LEI105 reduced 2-AG levels, but no change in substrate levels of DAGL was detected, which may suggest that DAG species are rapidly converted into other membrane constituents, such as phosphatidic acid by DAG-kinases (SI). Interestingly, arachidonic acid levels were reduced by LEI105 treatment of PC3 cells (SI). This may indicate that downstream metabolic pathways of 2-AG signaling are also affected and that the biosynthesis of 2-AG is the rate-limiting step. This is in line with a previously reported reduction of arachidonic acid levels in DAGL-α knockout mice and by KT-109 in mouse liver.[15,5]

LEI105 Reduces Synaptic Transmission in Hippocampus. To demonstrate a physiological effect of the inhibition of 2-AG biosynthesis by LEI105, we focused our attention on the hippocampal slice preparation in which depolarization-induced suppression of inhibition (DSI) is thought to be mediated via 2-AG-induced activation of presynaptic cannabinoid CB_1 receptors.[29,30] Experimental evidence, which supports a role of DAGL-α in DSI, has been obtained through the use of genetically engineered mice that constitutively lack DAGL-α. DSI was absent in these DAGL-α knockout mice, but not in their DAGL-β knockout counterparts.[5,10] Of note, anandamide levels were also reduced in these DAGL-α knockout mice. Acute DAGL inhibition studies with chemical tools would, therefore, provide an additional line of evidence to verify the role of DAGL-α in DSI. Pharmacological intervention studies with the two highly potent nonselective DAGL inhibitors, THL and OMDM-188, however, have challenged the unequivocal role of the DAGLs in DSI. Multiple groups reported a suppression of DSI by THL and/or OMDM-188,[31−36] whereas other groups did not find any inhibitory effect of THL and/or OMDM-188.[37,38] The discrepancy between the genetic model and the pharmacological studies led to the alternative hypothesis that 2-AG is released from preformed lipid stores instead of the "on demand" production of 2-AG.[39,40]

Here, we set out to investigate cannabinoid CB_1 receptor-dependent DSI in CA1 pyramidal neurons in hippocampal slices with our selective DAGL inhibitor. Preincubation and continuous application of 10 μM LEI105 had no effect on the amplitude of the stimulus-evoked inhibitory postsynaptic currents (IPSC) (271 ± 22 pA) compared to control (276 ± 32 pA). In control conditions, a DSI response could be evoked which decayed back with an exponential time course (τ = 34 s) to baseline levels. DSI was quantified as the reduction in IPSC amplitude averaged over the first 15 s after its induction. DSI evoked in slices treated with LEI105 was smaller than DSI induced in control slices (18 ± 7%, n = 15 and 36 ± 4%, n = 18, respectively; $p < 0.05$, Student's t test) (Figure 4). However, it is clear that DSI is not completely blocked in the presence of LEI105, which suggests that in addition to on demand 2-AG synthesis, the recruitment of 2-AG pools may contribute to DSI.[40] Alternatively, other endocannabinoids (e.g., anandamide) may be involved. Of note, at 10 μM LEI105 was still selective in our experimental set up and did not displace ^{3}H−CP55940 from the CB_1 receptor (SI), a result that excludes direct antagonism of the CB_1 receptor by LEI105. Thus, our data support the hypothesis of a major, but not exclusive, role of "on demand" production of 2-AG, which is responsible for the cannabinoid CB1 receptor-mediated synaptic plasticity.[33]

In conclusion, we have applied comparative and competitive chemproteomics using a tailor-made ABP (MB064) in combination with a broad-spectrum probe (TAMRA-FP) to identify and characterize the reversible DAGL inhibitor LEI105. This inhibitor was found to be an excellent tool to study the enzymatic role of DAGL-α in a neuronal setting and provides a critical counterpart to currently available DAGL knockout mice. This was exemplified in Neuro2A cells (where LEI105 reduced 2-AG levels, but not AEA levels) and in intact hippocampal brain slices (where a clear suppression of DSI was observed in the presence of LEI105). Using this combination of activity-based probes in a gel-based and chemoproteomic setting many lipases involved in the regulation of endocannabinoid levels (e.g., DAGL-α and β, ABHD6, ABHD12, MAGL, and FAAH) in the brain are targeted with high affinity. This opens the door to broadly apply this methodology to identify and characterize not only covalent irreversible inhibitors which can potentially lead to toxicity and immunogenicity of covalent inhibitor−protein complexes and selectivity issues using reactive covalent warheads, but also reversible inhibitors that target DAGL and other enzymes involved in 2-AG biosynthesis and metabolism. These reversible inhibitors have the additional intrinsic advantage to enable a better control of partial inhibition of their target enzyme. This is especially important with respect to endocannabinoid signaling in the CNS, since complete blockade of cannabinoid CB_1 receptor signaling in the CNS may lead to severe side effects.[41] Thus, this feature can play an important factor in the development of clinical candidates to provide therapeutic solutions for diseases, such as obesity, related metabolic disorders, and neuroinflammation, in which excessive 2-AG signaling or its metabolites play an important factor.

■ ASSOCIATED CONTENT

Supporting Information

Experimental procedures, supporting figures, compound characterization, and an appendix containing detailed proteomic data. The Supporting Information is available free of charge on the ACS Publications website at DOI: 10.1021/jacs.5b04883.

■ AUTHOR INFORMATION

Corresponding Author

*m.van.der.stelt@chem.leidenuniv.nl

Present Address

#Hsu Laboratories, Department of Chemistry, University of Virginia, McCormick Road, P.O. Box 400319, Charlottesville, Virginia 22904−4319, United States.

Notes

The authors declare no competing financial interest.

DOI: 10.1021/jacs.5b04883
J. Am. Chem. Soc. 2015, 137, 8851−8857

■ ACKNOWLEDGMENTS

We thank the Dutch Research Council-Chemical Sciences (ECHO-Grant: 711.014.009; MvdS), Leiden University, Faculty of Science ("Profiling Programme: Endocannabinoids"; MvdS, T.H., V.K.), and the Chinese Scholarship Council (DH) for financial support.

■ REFERENCES

(1) Katona, I.; Freund, T. F. *Ann. Rev. Neurosci.* **2012**, *35*, 529.
(2) Devane, W. A.; Hanus, L.; Breuer, A.; Pertwee, R. G.; Stevenson, L. A.; Griffin, G.; Gibson, D.; Mandelbaum, A.; Etinger, A.; Mechoulam, R. *Science* **1992**, *258*, 1946.
(3) Sugiura, T.; Kondo, S.; Sukagawa, A.; Nakane, S.; Shinoda, A.; Itoh, K.; Yamashita, A.; Waku, K. *Biochem. Biophys. Res. Commun.* **1995**, *215*, 89.
(4) Mechoulam, R.; Ben-Shabat, S.; Hanus, L.; Ligumsky, M.; Kaminski, N. E.; Schatz, A. R.; Gopher, A.; Almog, S.; Martin, B. R.; Compton, D. R.; Pertwee, R. G.; Griffin, G.; Bayewitch, M.; Barg, J.; Vogel, Z. *Biochem. Pharmacol.* **1995**, *50*, 83.
(5) Gao, Y.; Vasilyev, D. V.; Goncalves, M. B.; Howell, F. V.; Hobbs, C.; Reisenberg, M.; Shen, R.; Zhang, M. Y.; Strassle, B. W.; Lu, P.; Mark, L.; Piesla, M. J.; Deng, K.; Kouranova, E. V.; Ring, R. H.; Whiteside, G. T.; Bates, B.; Walsh, F. S.; Williams, G.; Pangalos, M. N.; Samad, T. A.; Doherty, P. *J. Neurosci.: Off. J. Soc. Neurosci.* **2010**, *30*, 2017.
(6) Di Marzo, V. *Nat. Rev. Drug Discovery* **2008**, *7*, 438.
(7) Blankman, J. L.; Cravatt, B. F. *Pharmacol. Rev.* **2013**, *65*, 849.
(8) Bisogno, T.; Howell, F.; Williams, G.; Minassi, A.; Cascio, M. G.; Ligresti, A.; Matias, I.; Schiano-Moriello, A.; Paul, P.; Williams, E. J.; Gangadharan, U.; Hobbs, C.; Di Marzo, V.; Doherty, P. *J. Cell Biol.* **2003**, *163*, 463.
(9) Reisenberg, M.; Singh, P. K.; Williams, G.; Doherty, P. *Philos. Trans. R. Soc. London. Ser. B, Biol. Sci.* **2012**, *367*, 3264.
(10) Tanimura, A.; Yamazaki, M.; Hashimotodani, Y.; Uchigashima, M.; Kawata, S.; Abe, M.; Kita, Y.; Hashimoto, K.; Shimizu, T.; Watanabe, M.; Sakimura, K.; Kano, M. *Neuron* **2010**, *65*, 320.
(11) Appiah, K. K.; Blat, Y.; Robertson, B. J.; Pearce, B. C.; Pedicord, D. L.; Gentles, R. G.; Yu, X. C.; Mseeh, F.; Nguyen, N.; Swaffield, J. C.; Harden, D. G.; Westphal, R. S.; Banks, M. N.; O'Connell, J. C. *J. Biomol. Screening* **2014**, *19*, 595.
(12) Janssen, F. J.; Deng, H.; Baggelaar, M. P.; Allara, M.; van der Wel, T.; den Dulk, H.; Ligresti, A.; van Esbroeck, A. C. M.; McGuire, R.; Di Marzo, V.; Overkleeft, H. S.; van der Stelt, M. *J. Med. Chem.* **2014**, *57*, 6610.
(13) Bisogno, T.; Mahadevan, A.; Coccurello, R.; Chang, J. W.; Allara, M.; Chen, Y.; Giacovazzo, G.; Lichtman, A.; Cravatt, B.; Moles, A.; Di Marzo, V. *Br. J. Pharmacol.* **2013**, *169*, 784.
(14) Ortar, G.; Bisogno, T.; Ligresti, A.; Morera, E.; Nalli, M.; Di Marzo, V. *J. Med. Chem.* **2008**, *51*, 6970.
(15) Hsu, K. L.; Tsuboi, K.; Adibekian, A.; Pugh, H.; Masuda, K.; Cravatt, B. F. *Nat. Chem. Biol.* **2012**, *8*, 999.
(16) Niphakis, M. J.; Cravatt, B. F. *Ann. Rev. Biochem.* **2014**, *83*, 341.
(17) Heal, W. P.; Dang, T. H.; Tate, E. W. *Chem. Soc. Rev.* **2011**, *40*, 246.
(18) Liu, Y.; Patricelli, M. P.; Cravatt, B. F. *Proc. Natl. Acad. Sci. U. S. A.* **1999**, *96*, 14694.
(19) Hoover, H. S.; Blankman, J. L.; Niessen, S.; Cravatt, B. F. *Bioorg. Med. Chem. Lett.* **2008**, *18*, 5838.
(20) Yang, P. Y.; Liu, K.; Ngai, M. H.; Lear, M. J.; Wenk, M. R.; Yao, S. Q. *J. Am. Chem. Soc.* **2010**, *132*, 656.
(21) Baggelaar, M. P.; Janssen, F. J.; van Esbroeck, A. C.; den Dulk, H.; Allara, M.; Hoogendoorn, S.; McGuire, R.; Florea, B. I.; Meeuwenoord, N.; van den Elst, H.; van der Marel, G. A.; Brouwer, J.; Di Marzo, V.; Overkleeft, H. S.; van der Stelt, M. *Angew. Chem., Int. Ed. Engl.* **2013**, *52*, 12081.
(22) Fowler, C. J. *Fundam. Clin. Pharmacol.* **2006**, *20*, 549.
(23) Boger, D. L.; Sato, H.; Lerner, A. E.; Hedrick, M. P.; Fecik, R. A.; Miyauchi, H.; Wilkie, G. D.; Austin, B. J.; Patricelli, M. P.; Cravatt, B. F. *Proc. Natl. Acad. Sci. U. S. A.* **2000**, *97*, 5044.
(24) Pedicord, D. L.; Flynn, M. J.; Fanslau, C.; Miranda, M.; Hunihan, L.; Robertson, B. J.; Pearce, B. C.; Yu, X. C.; Westphal, R. S.; Blat, Y. *Biochem. Biophys. Res. Commun.* **2011**, *411*, 809.
(25) van der Wel, T.; Janssen, F. J.; Baggelaar, M. P.; Deng, H.; den Dulk, H.; Overkleeft, H. S.; van der Stelt, M. *J. Lipid Res.* **2015**, *56*, 927.
(26) Mileni, M.; Garfunkle, J.; DeMartino, J. K.; Cravatt, B. F.; Boger, D. L.; Stevens, R. C. *J. Am. Chem. Soc.* **2009**, *131*, 10497.
(27) Bachovchin, D. A.; Ji, T.; Li, W.; Simon, G. M.; Blankman, J. L.; Adibekian, A.; Hoover, H.; Niessen, S.; Cravatt, B. F. *Proc. Natl. Acad. Sci. U. S. A.* **2010**, *107*, 20941.
(28) Jung, K. M.; Astarita, G.; Thongkham, D.; Piomelli, D. *Mol. Pharmacol.* **2011**, *80*, 60.
(29) Ohno-Shosaku, T.; Maejima, T.; Kano, M. *Neuron* **2001**, *29*, 729.
(30) Wilson, R. I.; Nicoll, R. A. *Nature* **2001**, *410*, 588.
(31) Hashimotodani, Y.; Ohno-Shosaku, T.; Kano, M. *J. Neurosci.: Off. J. Soc. Neurosci.* **2007**, *27*, 1211.
(32) Hashimotodani, Y.; Ohno-Shosaku, T.; Maejima, T.; Fukami, K.; Kano, M. *Neuropharmacology* **2008**, *54*, 58.
(33) Hashimotodani, Y.; Ohno-Shosaku, T.; Tanimura, A.; Kita, Y.; Sano, Y.; Shimizu, T.; Di Marzo, V.; Kano, M. *J. Physiol.* **2013**, *591*, 4765.
(34) Edwards, D. A.; Zhang, L. H.; Alger, B. E. *Proc. Natl. Acad. Sci. U. S. A.* **2008**, *105*, 8142.
(35) Zhang, L. H.; Wang, M. N.; Bisogno, T.; Di Marzo, V.; Alger, B. E. *PLoS One* **2011**, 6.
(36) Szabo, B.; Urbanski, M. J.; Bisogno, T.; Di Marzo, V.; Mendiguren, A.; Baer, W. U.; Freiman, I. *J. Physiol.-London* **2006**, *577*, 263.
(37) Edwards, D. A.; Kim, J.; Alger, B. E. *J. Neurophysiol.* **2006**, *95*, 67.
(38) Min, R.; Testa-Silva, G.; Heistek, T. S.; Canto, C. B.; Lodder, J. C.; Bisogno, T.; Di Marzo, V.; Brussaard, A. B.; Burnashev, N.; Mansvelder, H. D. *J. Neurosci.* **2010**, *30*, 2710.
(39) Min, R.; Di Marzo, V.; Mansvelder, H. D. *Neuroscientist: Rev. J. Bring. Neurobiol., Neurol., Psych.* **2010**, *16*, 608.
(40) Alger, B. E.; Kim, J. *Trends Neurosci.* **2011**, *34*, 304.
(41) Kunos, G.; Tam, J. *Br. J. Pharmacol.* **2011**, *163*, 1423.

DOI: 10.1021/jacs.5b04883
J. Am. Chem. Soc. 2015, 137, 8851−8857